

Evolution and decay of an active region: Magnetic shear, flare and CME activity

C. H. Mandrini¹, L. van Driel-Gesztelyi^{2,3}, B. Thompson⁴, S. Piontke⁵, P. Démoulin² and G. Aulanier²

¹ Instituto de Astronomía y Física del Espacio, IAFE, Argentina

² Observatoire de Paris, DASOP, Meudon Cédex, France

³ Konkoly Observatory, Budapest, Hungary

⁴ NASA/GSFC, Greenbelt, U.S.A.

⁵ USRA, Naval Research Laboratory, Washington, DC, USA.

Received: November 6, 1998; accepted: April 12, 1999.

RESUMEN

Desde abril de 1996 y hasta febrero de 1997, se observó en el disco solar un complejo de actividad. Este complejo exhibió su nivel más alto de actividad durante el nacimiento de la región activa (AR) 7978. Nuestro análisis se extiende a lo largo de seis rotaciones solares, desde la aparición de AR 7978 (julio de 1996) hasta el decaimiento y dispersión de su flujo (noviembre de 1996). Los datos en varias longitudes de onda provistas por los instrumentos a bordo del Solar and Heliospheric Observatory (SOHO) y del satélite japonés *Yohkoh*, nos permiten seguir la evolución de la región desde la fotosfera hasta la corona. Usando los magnetogramas del disco completo obtenidos por el Michelson Doppler Imager (SOHO/MDI) como condiciones de contorno, calculamos el campo magnético coronal y determinamos su apartamiento de la potencialidad ajustando las líneas de campo calculadas a los arcos observados en rayos X blandos. Discutimos la evolución de la torsión del campo magnético coronal y su probable relación con la actividad observada en forma de eyecciones de masa coronal (CMEs) y fulguraciones.

PALABRAS CLAVE: Actividad solar, eyecciones de masa coronal, fulguraciones, campo magnético coronal.

ABSTRACT

An activity complex was observed on the solar disk between April, 1996 and February, 1997 that reached its highest level of activity during the birth of AR 7978. Our observations extend over six solar rotations, from the emergence of AR 7978 (July 1996) until the decay and dispersion of its flux (November 1996). Multi-wavelength observations, provided by instruments aboard the Solar and Heliospheric Observatory (SOHO) and the Japanese spacecraft *Yohkoh*, follow the evolution of the region from the photosphere to the corona. Using full disk magnetograms obtained by the Michelson Doppler Imager (SOHO/MDI) as boundary condition, we calculate the coronal magnetic field and determine its shear by fitting the computed field lines to the observed soft X-ray loops. We discuss the evolution of the coronal field shear and its probable relation to flare and coronal mass ejection activity.

KEY WORDS: Solar activity, coronal mass ejections, flares, coronal magnetic field.

1. INTRODUCTION

Large flares and coronal mass ejections are produced in regions where the magnetic shear is high along the longitudinal inversion line (Heyvaerts and Hagyard 1991, and references therein). Rust (1994) studied the correspondence between the helicity sign in magnetic clouds observed at 1AU, and the predominant chirality in the hemisphere where the probable precursor solar event occurred. He speculated that solar flares and CMEs may be necessary to purge magnetic helicity from each hemisphere. On the other hand, magnetohydrodynamic (MHD), simulations, both ideal and resistive, have shown that magnetic shear in the case of arcades (Mickic and Linker 1994, Amari *et al.*, 1996a) or twist in the case of flux tubes (Amari *et al.*, 1996b) lead to expansion of the field followed by partial opening of the configuration.

Lin *et al.* (1998) have shown analytically that the curvature force acting on a flux rope can help to drive it outward from the Sun. Initially the flux rope can be suspended in the corona by a balance between magnetic tension, compression and curvature forces, but this balance can be lost if the photospheric sources of the magnetic field slowly decay with time. In this model, the loss of ideal MHD equilibrium cannot completely open the field, but it can lead to the sudden formation of a current sheet and, if rapid reconnection occurs in this sheet, then the flux rope can escape from the Sun. These studies suggest that evolution of the observed magnetic field and its shear are related to the production of flares and CMEs and constrain the main causes of these phenomena.

Solar activity during the second half of 1996 was governed by an activity complex located in the southern hemi-

sphere. The most outstanding active region (AR) in this complex was AR 7978. The first well-formed sunspots of the AR were seen on July 6, 1996, though emergence of new flux at that latitude could be traced as early as April, 1996 (Harvey and Hudson 1997). From July 1996, and for the next five solar rotations (November, 1996), only a few, short-lived and small ARs were observed on the disk. Thus solar activity at that period came from this AR, and a straightforward comparison between the evolution of the magnetic field intensity and shear in the region and flare and CME production can be made. In Section 2 we present observations of the region at different atmospheric layers, described their global evolution, and we summarize the observed flare and CME activity. The magnetic field model and the study of the magnetic shear evolution is presented in Section 3. We summarize our results and conclusions in Section 4.

2. OBSERVATIONS

Figure 1 shows the total 1 - 8 Å (GOES 9, low channel) solar flux from the appearance of AR 7978 and during its decay. The evolution of the GOES flux represents the global decrease in brightness of the region. AR 7978 was the only major active region present in the solar disk, as can be noticed from the sharp decrease in the GOES flux due to its occultation. During July, the soft X-ray intensity is high and the numerous observed spikes correspond to the flares occurring during that rotation. As the AR decays and the magnetic flux starts to disperse, the intensity of the spikes associated to flares diminishes. On the other hand, the global trend of the GOES curve is such that the flux decreases by almost two orders of magnitude from July to October, 1996 (van Driel-Gesztelyi 1998).

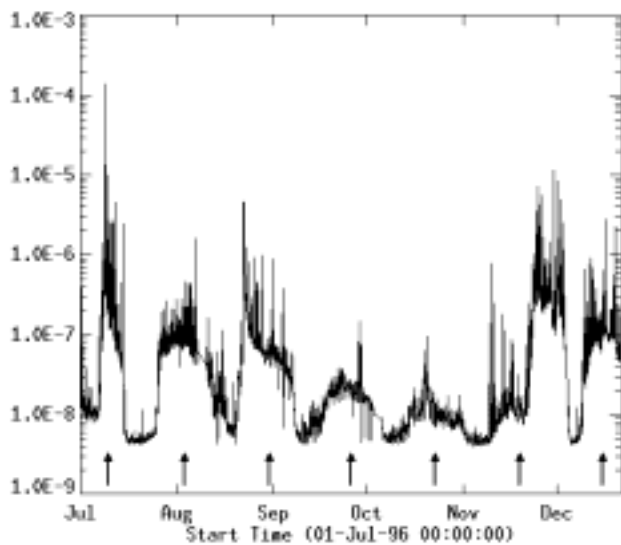


Fig. 1. Evolution of the 1 - 8 Å total flux irradiance (W/m^2) of the Sun along six months (GOES 9 data). The arrows indicate CMP of AR 7978.

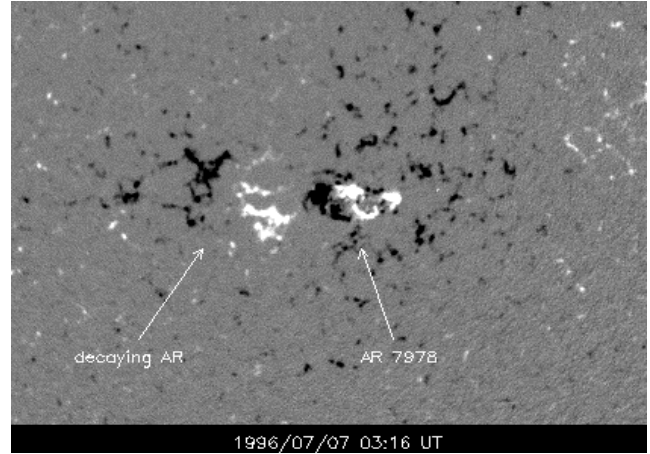


Fig. 2. SOHO/MDI magnetic map obtained on July 7, 1996. AR 7978 (to the West) emerges in the presence of an old decaying bipole (to the East). The data above ± 100 G have been saturated. North is up and West is to the right. The size of the box is 605 Mm and 430 Mm in the horizontal and vertical directions, respectively.

Figures 2 to 5 illustrate the evolution of the AR at different atmospheric layers. The images correspond to successive central meridian passages (CMPs), pointed out by arrows in Figure 1. Strong emergence of flux was observed at S10 E31 from July 4, 1996, which we will call the first rotation. This was the birth of AR 7978. The new flux appeared west of an old and decayed bipolar region as shown in the SOHO/MDI magnetic map of Figure 2. Between the first and second rotations the old positive flux, closer to the newly emerged region, is completely swept out by the new negative flux (compare Figure 2 to Figure 3a). Figures 3a to 3f show the decrease of the magnetic field intensity and the dispersion of flux concentrations during the next six rotations from August to December, 1996. By the fourth rotation (September, 1996) sunspots have disappeared in the AR. The diffusion of the field is evident in Figures 3, as well as the rotation of the inversion line by $\approx 45^\circ$, partly due to differential rotation. By December, the dominant preceding polarity can still be recognized. All along the diffusion of the bipolar flux, any polarity with opposite sign to the corresponding main field rapidly disappears, probably due to flux cancellation processes.

Figure 4 corresponds to images obtained by the Extreme Ultraviolet Image Telescope (EIT, on board SOHO) in He II, 304 Å. These images show the evolution of the AR in the transition region. As the area of the plage increases following the dispersion of the flux, its intensity decreases. No trances of filaments are seen at the early stages; by the fourth rotation, a quiescent filament is located along the inversion line. Rotation by rotation it increases in length and bends as the inversion line rotates. Figure 5 from the Soft X-ray Telescope (SXT, On board *Yohkoh*) shows the decay of the AR at coronal heights. Two aspects are relevant in this figure: first,

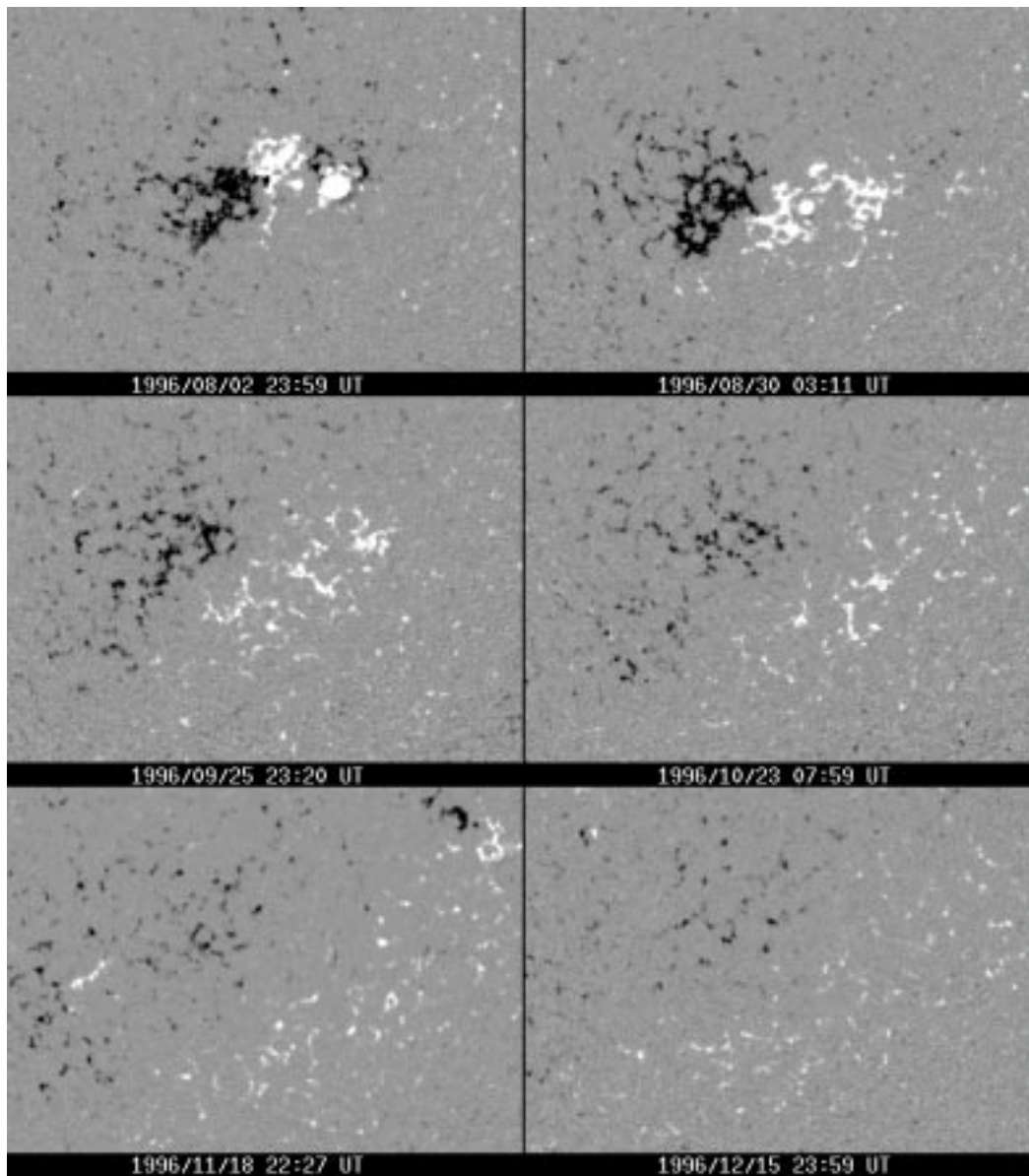


Fig. 3. SOHO/MDI maps showing the distribution of the magnetic field in AR 7978 at successive CMPs from the second to the seventh rotation. The convention is the same as in Fig. 2.

the decrease in the brightness of the loops, and second, the apparent increase of the magnetic shear at coronal heights from the second to at least the fourth rotation.

Beginning with the emergence of AR 7978 and for at least the next two rotations, the AR produced numerous flares including an X2.6 flare and CME event on July 9, (see Dryer *et al.*, 1998). The spots disappeared by September (see Figures 1 and 3). On the other hand, CME activity, at first related to flare events, continued at a high level for the next three rotations. This late CME activity (see van Driel-Gesztelyi *et al.*, 1998) was observed at the time when the coronal magnetic shear, as indicated by SXT loops, reached its maximum (see also next Section). Table 1 illustrates the

Table 1

Flare and CME activity

| Date CMP | X flares | M flares | C flares | B flares | CMEs |
|------------|----------|----------|----------|----------|------|
| 07 July | 01 | 02 | 14 | 11 | 04 |
| 02 August | - | - | - | 16 | 08 |
| 30 August | - | - | 01 | 08 | 07 |
| 25 Sept. | - | - | - | - | 03 |
| 23 October | - | - | - | - | 04 |
| 18 Nov. | - | - | - | - | 06 |
| 16 Dec. | - | - | - | - | 06 |

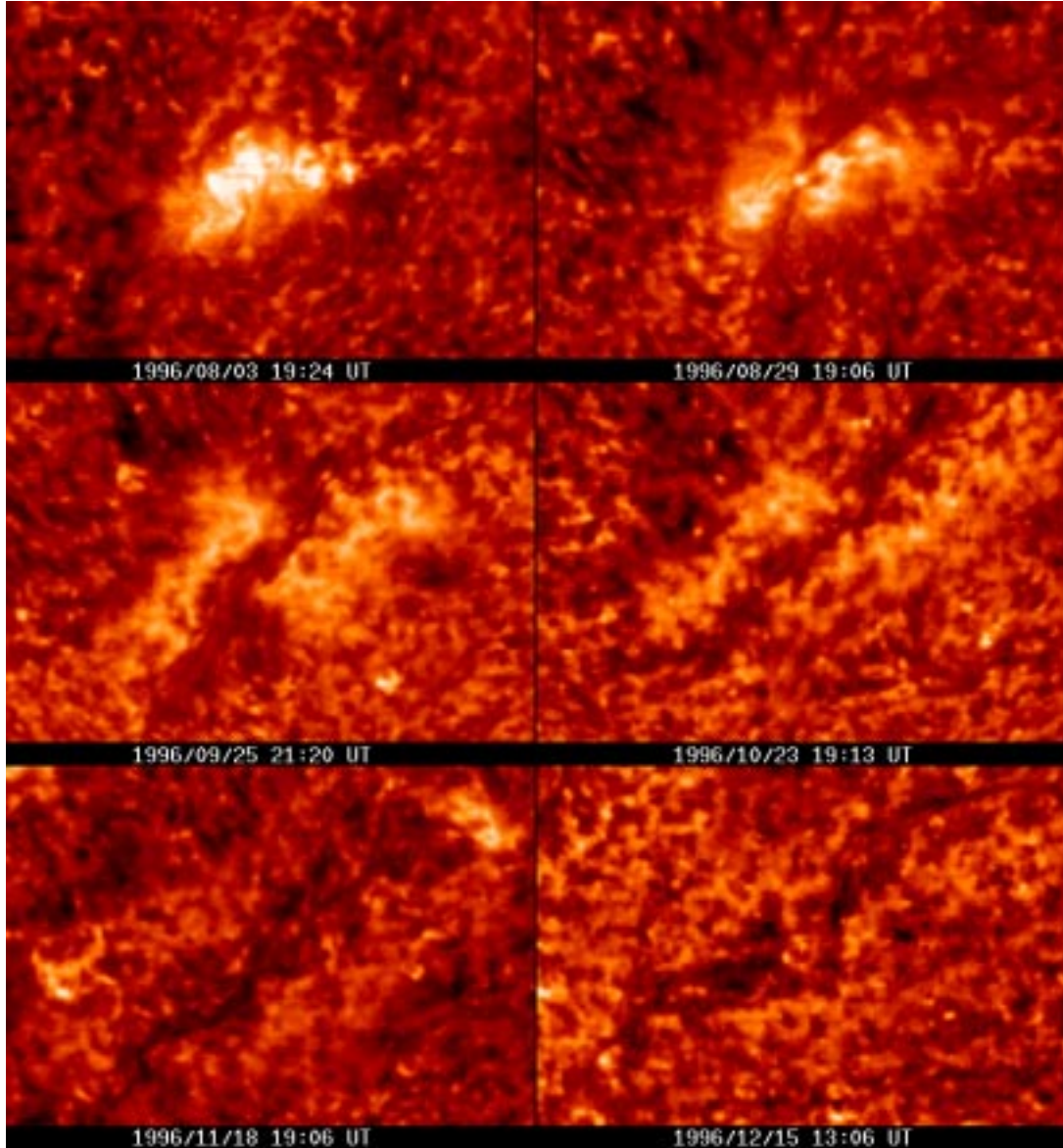


Fig. 4. SOHO/EIT images in HeII 304 Å illustrating the evolution of AR 7978 in the transition region (T^a 80000 K). The images are co-aligned with the magnetic maps in Fig. 3.

flare and CME from the second to the fifth column, and the number of CMEs associated with the AR. The data sources of Table 1 are the production. We have listed the CMP date for each rotation in the first column, the number and importance of the flares GOES X-ray and optical event catalog (see <http://www.lmsal.com/SXT/operations.html>), and the SOHO/EIT and SOHO/LASCO observations analyzed by us (for the LASCO CME list see <http://lasco-www.nrl.navy.mil/cmelist.html>).

3. MAGNETIC FIELD MODEL

We model the magnetic field of the AR along six rotations by the linear force free approach ($\nabla \times \mathbf{B} = \alpha \mathbf{B}$, α con-

stant), using the extrapolation method in Démoulin et al. (1997). MDI magnetic field maps at CMP have been used as boundary conditions.

The free parameter α was found by fitting the shape of the observed soft X-ray loops. Not all SXT loops at a given CMP can be represented by the same value of α ; in all cases a shear gradient exists in the North - South direction. Figures 6 and 7 show the overlays between the computed field lines and SXT loops illustrating the magnetic shear evolution. Within the limitations of our approach, considering only the coronal shear, Figure 6 shows that AR 7978 emerged as non-potential ($\alpha \approx 0.01 \text{ } 10^{-2} \text{ Mm}^{-1}$) with the helicity sign corresponding to the southern hemisphere (Pevtsov et al., 1995).

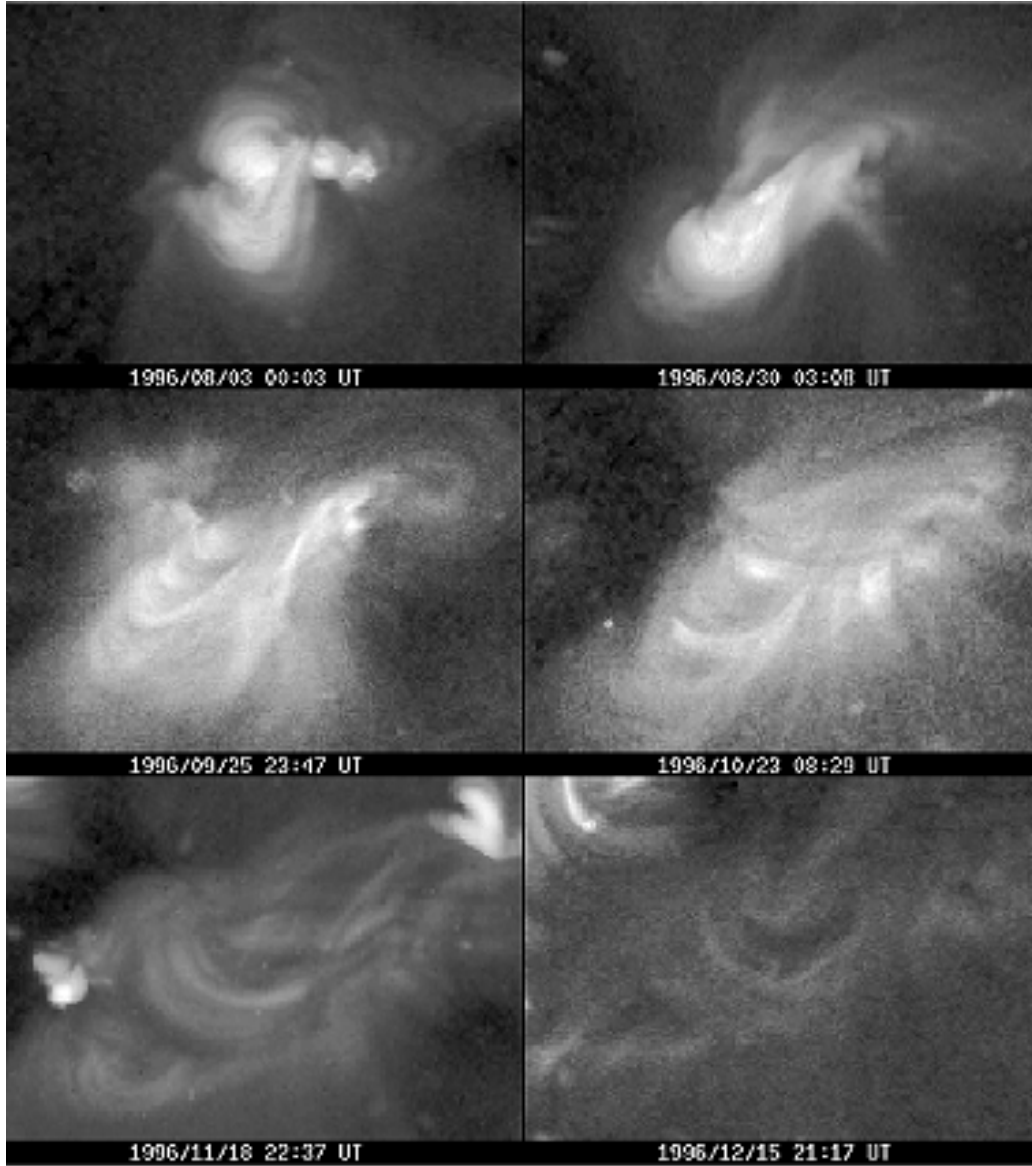


Fig. 5. *Yohkoh*/SXT images following the evolution of AR 7978 at coronal heights (1.5 to 5.10⁶K). The images are co-aligned with the corresponding images in Figs. 3 and 4.

It was very close to a preexisting bipole that had a higher opposite sign helicity ($\alpha \approx -0.05 \cdot 10^{-2} \text{ Mm}^{-1}$). Figure 7 corresponds to the second rotation and illustrates the variation of α from North to South.

Table 2 list the values of α from the second to the sixth rotation. In addition to the shear gradient, the shear increases from the first to the fourth rotation and seems to saturate or decrease by the sixth rotation.

4. DISCUSSION AND CONCLUSIONS

We have described a typical scenario for the decay of active regions (see van Driel-Gesztelyi, 1998) at different

Table 2

Evolution of the magnetic shear

| Date | α - North (10^{-2} Mm^{-1}) | α - South (10^{-2} Mm^{-1}) |
|--------------|---|---|
| 02 August | 0.75 | 0.30 |
| 30 August | 1.10 | 0.75 |
| 25 September | 1.40 | 1.00 |
| 23 October | 1.40 | 0.90 |
| 18 November | - | 0.90 |

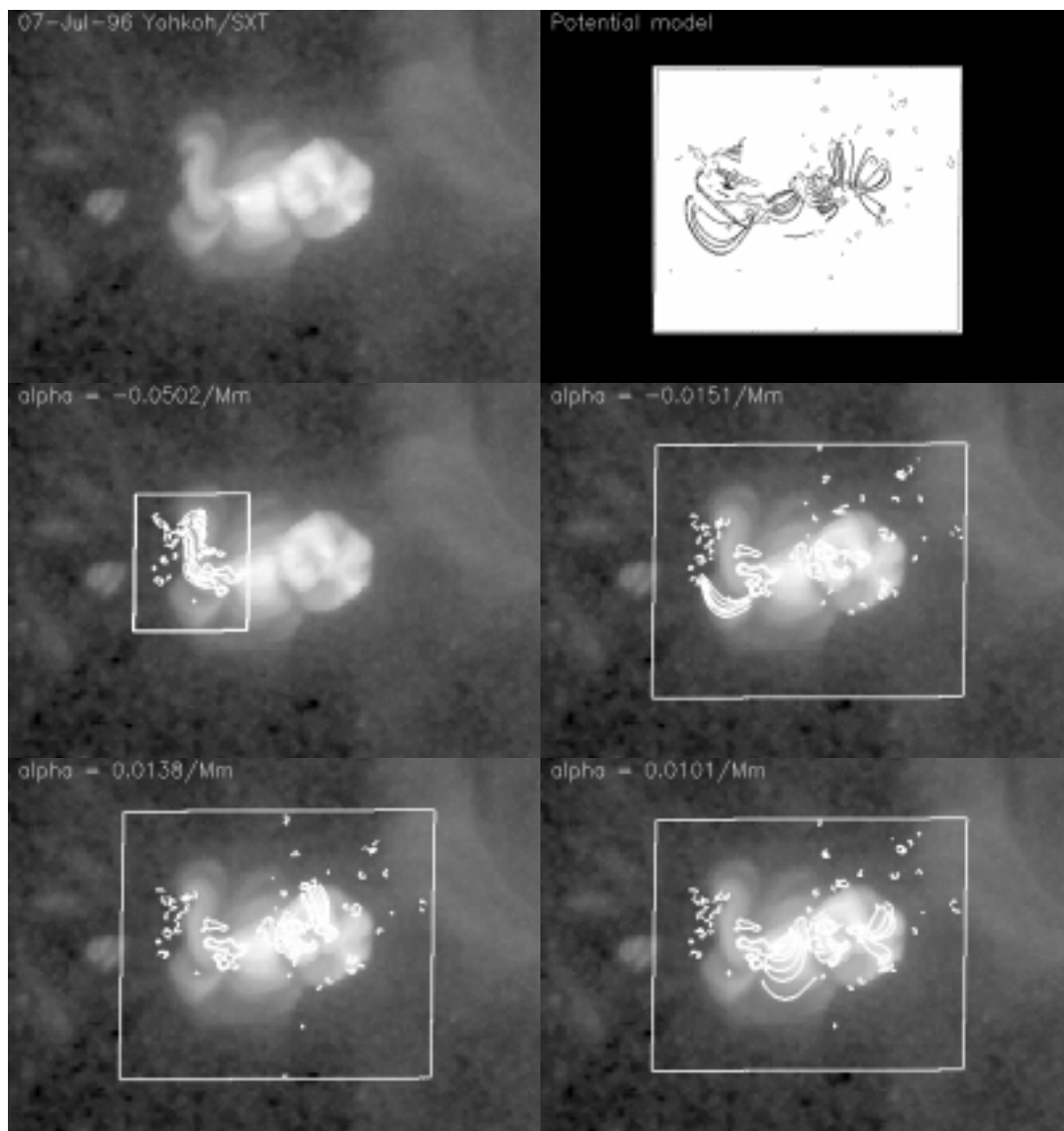


Fig. 6 Computed magnetic field lines overlying the observed *Yohkoh*/SXT loops. In all the figures the value of α used in the magnetic field model is indicated. The top right figure shows the X-ray loops, while the figure to the left corresponds to a potential field model of the region, shown for comparison. We have drawn isocontours of the line of sight component of the field corresponding to $\pm 50, 100, 400$ G with a continuous (dashed) line for the positive (negative) values. The figures in the second row correspond to the model to the old bipole existing at the time of the emergence of AR 7978. The other figures show the model for AR 7978 in its early growing phase. These two regions have opposite sign helicity.

levels in the solar atmosphere. Since this AR is the only one in the solar disk along several months, we are able to associate the long-term evolution of the field with different manifestations of coronal activity.

The emergence of AR 7978, interacting through flux cancellation with the pre-existing region of opposite sign helicity, may be the cause of the intense flare and CME activity observed during the first and second rotations. Flare activity decreases and disappears after the magnetic flux has dispersed, so that no spots are observed after the third rotation. On the other hand, magnetic shear increases up to the

fourth rotation, presumably due to twisted flux emergence and differential rotation. CME activity persists at a high level as long as the magnetic field shear increases, and even afterwards. Even though the effect of differential rotation and emergence of twisted flux has not ceased after the fourth rotation, we find that the shear reaches a certain value and even starts decreasing by the sixth rotation.

Thus enough magnetic free energy in a given volume, plus an appropriate photospheric field evolution to create a complex magnetic field topology, are needed for flaring. If a filament is present, it can be destabilized and an eruption

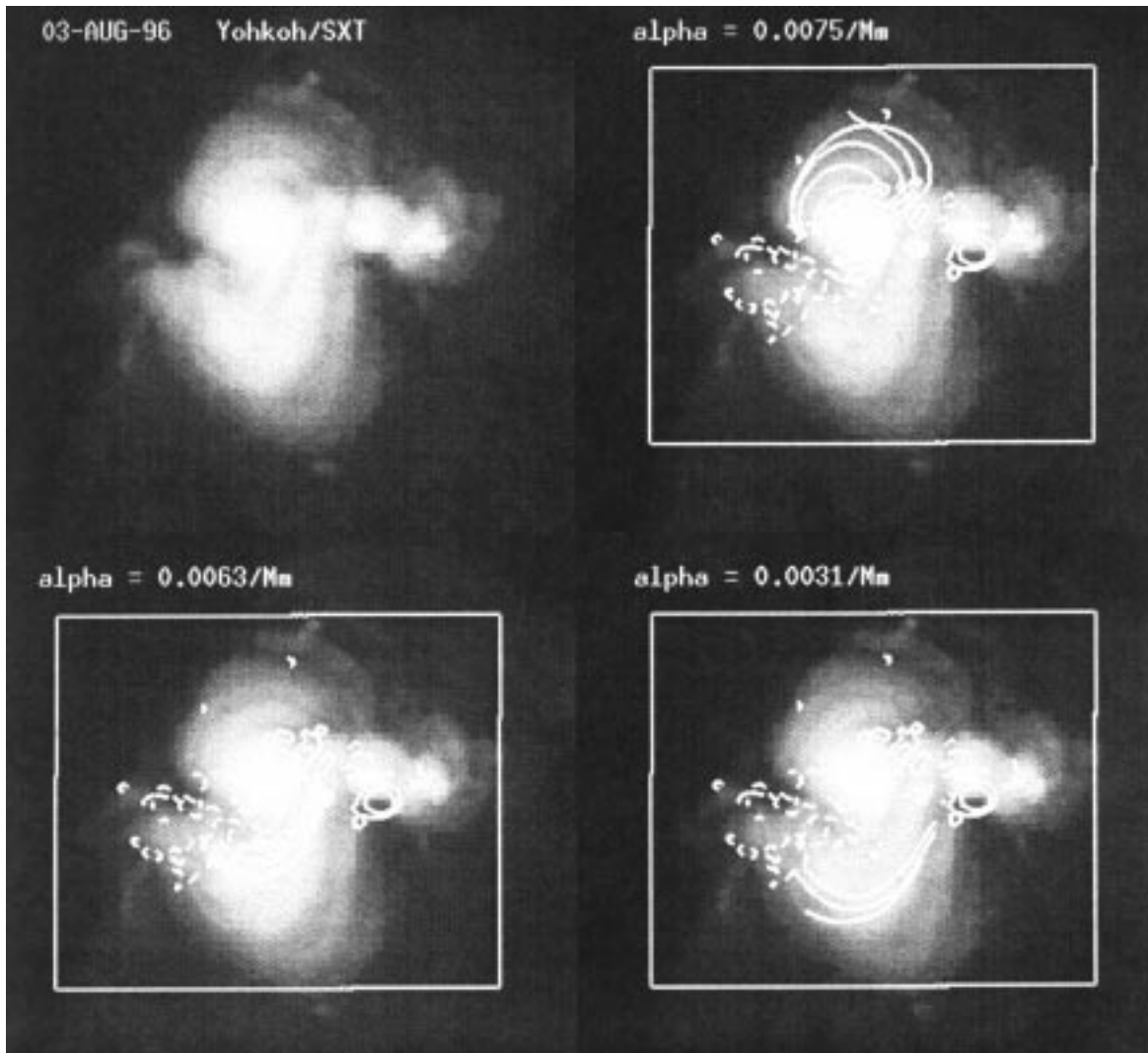


Fig. 7. Idem Fig. 6 for the second rotation. Notice the North - South shear gradient.

occurs. This may be the origin of flares and CMEs in the early stages of the AR. Late CMEs may be launched by magnetic shear or twist above a certain value in the whole configuration. The decrease in the intensity of the photospheric field may also contribute, as suggested by some numerical and analytical models mentioned in the Introduction. Late CMEs may be a mechanism by which the Sun sheds an excess of magnetic twist and shear beyond a given threshold.

ACKNOWLEDGEMENTS

We thank the Yohkoh Team and the MSSL YDAC for the Yohkoh/SXT data, and the SOHO/MDI and SOHO/EIT consortium for the magnetic and UV data respectively. This work benefitted from discussions and data analysis during the 2nd SOHO-Yohkoh CDAW, held in MEDOC-SOHO Data Center, Orsay, France. PD and CHM acknowledge financial support from ECOS (France) and SECYT (Argen-

tina) through the cooperative science program A97U01. LvDG acknowledges the Hungarian Government grants OTKA T-026165 and AKP 97-58 2,2. CHM, a member of the Carrera del Investigador Científico (CONICET), thanks CONICET for grant PEI 104/98.

BIBLIOGRAPHY

- AMARI, T., J. F. LUCIANI, J. J. ALY and M. TAGGER, 1996a. Plasmoid formation in a single sheared arcade and application to coronal mass ejections. *Astron. Astrophys.*, *306*, 913-923.
- AMARI, T., J. F. LUCIANI, J. J. ALY and M. TAGGER, 1996b. Very fast opening of a three-dimensional twisted magnetic flux tube. *Astrophys. J.*, *466*, L39-L42.
- DEMOULIN, P., L. G. BAGALA, C. H. MANDRINI, J. C. HENOUX and M. G. ROVIRA, 1997. Quasi-separatrix

- layers in solar flares II. Observed magnetic configurations. *Astron. Astrophys.*, 325, 305-317.
- DRYER, M., M. D. ANDREWS, H. AURASS et al., 1998. The solar minimum active region 7978, its X2.6/1B flare, CME, and interplanetary shock propagation of 9 July 1996. *Solar Phys.*, 181, 159-183.
- HARVEY, K. L. and H. S. HUDSON, 1997. The formation and evolution of the coronal holes associated with NOAA region 7978. *In: Observational Plasma Astrophysics: Five Years of Yohkoh and Beyond*, T. Watanabe, T. Kosugi, A. C. Sterling (eds.), Kluwer, 315.
- HAYVAERTS, J. and M. J. HAGYARD, 1991. On the energy storage in solar flares. *In: Proc. of the Flares 22 Workshop, Dynamics of Solar Flares*, B. Schmieder and E. Priest (eds.), Paris Obs., 1.
- LIN, J., T. G. FORBES, P. A. ISENBERG and P. DEMOULIN, 1998. The effect of curvature on flux-rope models of coronal mass ejections. *Astrophys. J.*, 504, 1006-1019.
- MIKIC, Z. and J. A. LINKER, 1994. Disruption of coronal magnetic field arches. *Astrophys. J.*, 430, 898-912.
- PEVTSOV, A. A., R. C. CANFIELD and T. R. METCALF, 1995. Latitudinal variation of helicity of photospheric magnetic fields. *Astrophys. J.*, 440, L109-L112.
- RUST, D. M., 1994. Spawning and shedding helical magnetic fields in the solar atmosphere. *Geophys. Res. Lett.*, 21, 241-244.
- VAN DRIEL-GESZTELYI, L., 1998. Evolution and decay of active regions. *In: Three Dimensional Structure of Solar Active Regions*, Proc. 2nd ASPE, C. Alissandrakis and B. Schmieder (eds.), ASP Conf. Ser., 155, 202-223.
- VAN DRIEL-GESZTELYI, L., B. SCHMIEDER, G. AULANIER et al., 1998. Filament disappearance brusque and CME - September 25-26, 1996 event. *In: D. Webb, D. Rust and B. Schmieder (eds.) New Perspectives on Solar Prominences*. IAU Coll. 167, ASP Conference Series, Vol. 150, 366.
-
- C. H. Mandrini¹, L. van Driel-Gesztelyi^{2,3}, B. Thompson⁴, S. Punkett⁵, P. Démoulin² and G. Aulanier²
- ¹ Instituto de Astronomía y Física del Espacio, IAFE, CC.67, Suc. 28, 1428 Bs. As., Argentina.
- ² Observatoire de Paris, DASOP, IRA2080 (CNRS), 92195 Meudon Cédex, France.
- ³ Konkoly Observatory, Budapest, Pf. 67, H-1525, Hungary.
- ⁴ NASA/GSFC, Greenbelt, MD 20771, U.S.A.
- ⁵ USRA, Naval Research Laboratory, Washington, DC, 20375, USA.